Non-Maxwellian behavior and quasistationary regimes near the modal solutions of the Fermi-Pasta-Ulam β system

M. Leo[*] and R. A. Leo[†]

Dipartimento di Matematica e Fisica "Ennio De Giorgi", Università del Salento, Via per Arnesano, 73100 Lecce, Italy

P. Tempesta[‡]

Departamento de Física Teórica II, Facultad de Físicas, Ciudad Universitaria, Universidad Complutense, 28040 Madrid, Spain

C. Tsallis[§]

Centro Brasileiro de Pesquisas Fisicas and National Institute of Science and Technology for Complex Systems, Rua Xavier Sigaud 150, 22290-180 Rio de Janeiro, Rio de Janeiro, Brazil and Santa Fe Institute, 1399 Hyde Park Road, Santa Fe, New Mexico 87501, USA

In a recent paper [M. Leo, R. A. Leo, and P. Tempesta, J. Stat. Mech. (2011) P03003], it has been shown that the $\pi/2$-mode exact nonlinear solution of the Fermi-Pasta-Ulam β system, with periodic boundary conditions, admits two energy density thresholds. For values of the energy density ϵ below or above these thresholds, the solution is stable. Between them, the behavior of the solution is unstable, first recurrent and then chaotic. In this paper, we study the chaotic behavior between the two thresholds from a statistical point of view, by analyzing the distribution function of a dynamical variable that is zero when the solution is stable and fluctuates around zero when it is unstable. For mesoscopic systems clear numerical evidence emerges that near the second threshold, in a large range of the energy density, the numerical distribution is fitted accurately with a q-Gaussian distribution for very large integration times, suggesting the existence of a quasistationary state possessing a weakly chaotic behavior. A normal distribution is recovered in the thermodynamic limit.

I. INTRODUCTION

In recent decades, the study of Hamiltonian many-body systems has undergone great development. These systems are indeed ubiquitous in many different fields of science. In this context, one of the most remarkable examples is provided by the Fermi-Pasta-Ulam (FPU) system [1]. It has been intensively studied since its proposal (see [2] for a recent review), and still represents an invaluable model for studying nonlinear phenomena.

A recent series of papers [3–7] has been devoted to the stability properties of an interesting class of solutions admitted by the FPU β system with periodic boundary conditions: the *one-mode solutions* (OMSs) [8–10]. These are exact solutions, usually referred to by means of the values of the mode number $n = \frac{N}{4}, \frac{N}{3}, \frac{N}{2}, \frac{2}{3}N, \frac{3}{4}N$, where N is the number of particles of the system. These modes are named equivalently (as in the present paper) $\pi/2, 2\pi/3, \pi$, etc. Their stability has also been analyzed in [11,12].

In [3], the existence of a new stability threshold $\epsilon_2(N)$, apart from the well-known one of low energy $\epsilon_1(N)$, was discovered for the $\pi/2$ mode. Indeed, on increase of the energy density ϵ, the system experiences an abrupt transition from the region of chaotic behavior to a region where the nonlinear mode solution again becomes stable. Technically, we have used a global indicator introduced in [3,6], i.e., the ratio ρ between the standard deviation and the first moment of the absolute value

of the relevant variable for a given probability distribution. For a Gaussian distribution, $\rho = \sqrt{\pi/2}$. This indicator estimates the deviation of a generic assigned distribution from Gaussian behavior for any value of the excitation energy density. It is a function of the dynamical variables of the configuration space only and its usefulness relies on the fact that is model independent. By means of this indicator, in [3,6] we studied the stability of the π and $\pi/2$ modes as functions of the energy density.

Figure 1 shows a typical curve of stability of the OMS $\pi/2$ for $N = 128$. The time of stability of the mode is plotted as a function of ϵ; the existence of the two thresholds ϵ_1 and ϵ_2 is evident: below ϵ_1 and above ϵ_2 the time of stability tends to infinity.

The aim of this work is to explore the statistical properties of the FPU β chain, following the orbits of the $\pi/2$ mode. A connection between the weakly chaotic dynamics of the model and nonextensive statistical mechanics was first established in [6] in the specific case of the π mode, for initial conditions in a narrow region of the phase space. This result has also been confirmed, for the same modal solution, by a subsequent analysis [13].

Here we exhibit striking evidence of the existence, for the $\pi/2$ mode, of *quasistationary states* whose thermostatistics is governed by a long standing q-Gaussian distribution for a considerable range of the energy density. This is achieved by performing an accurate analysis of a set of suitable observables associated with the evolution of the system. More precisely, for values of the energy density between ϵ_1 and ϵ_2, up to values very close to ϵ_2, the numerical distribution is fitted with a high accuracy by a q-Gaussian distribution, for values of N approximately up to 100, and very large integration times.

[*]mario.leo@le.infn.it
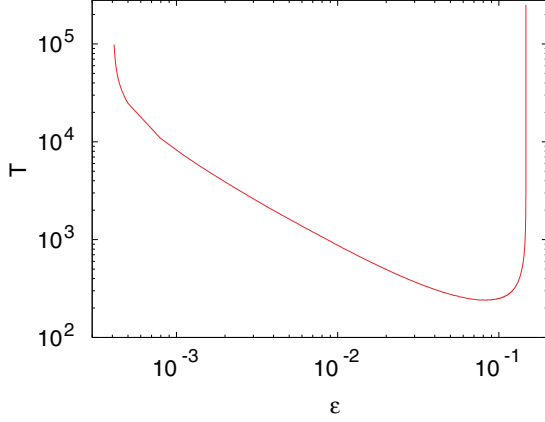[†]leora@le.infn.it
[‡]p.tempesta@fis.ucm.es
[§]tsallis@cbpf.br

FIG. 1. (Color online) Stability time T for the OMS $\pi/2$ ($N = 128$) vs ϵ: it is defined as the time (divided by π) after which the ratio between the energy of the mode and its initial energy is less than 0.999 99.

Interestingly enough, the distributions found in our analysis are extremely stable, i.e., they remain q-Gaussian without converting into a Gaussian, or any different distribution. For N very large, q approaches 1, hence the q-Gaussian distribution essentially recovers the normal one.

II. QUASISTATIONARY STATES IN WEAKLY CHAOTIC REGIMES

Quasistationary states have been observed in different Hamiltonian systems [14]. For the Hamiltonian mean-field model, discussed in [15] and describing a system of classical coupled rotors, numerical evidence was found of the existence of out-of-equilibrium quasistationary states, having a lifetime that increases with the number of particles N of the system. Also, in [13] this kind of state has been recognized in weakly chaotic regimes of several multidimensional Hamiltonian dynamics.

For the sake of clarity, let us now briefly recall the main features of the FPU β system with N oscillators and periodic conditions. By denoting with x_i and p_i the coordinates and the associated momenta, the Hamiltonian reads

$$H = \frac{1}{2}\sum_{i=1}^{N} p_i{}^2 + \frac{1}{2}\sum_{i=1}^{N}(x_{i+1} - x_i)^2 + \frac{\beta}{4}\sum_{i=1}^{N}(x_{i+1} - x_i)^4$$

with $x_{N+1} = x_1$ and $\beta \geqslant 0$. All quantities are dimensionless. In terms of the normal coordinates Q_i and P_i, defined by the relations

$$Q_i = \sum_{j=1}^{N} S_{ij}x_j, \qquad P_i = \sum_{j=1}^{N} S_{ij}p_j, \tag{1}$$

with

$$S_{ij} = \frac{1}{\sqrt{N}}\left(\sin\frac{2\pi ij}{N} + \cos\frac{2\pi ij}{N}\right), \tag{2}$$

the harmonic energy of the mode i is

$$E_i = \tfrac{1}{2}\left(P_i^2 + \omega_i^2 Q_i^2\right), \tag{3}$$

where for periodic boundary conditions

$$\omega_i^2 = 4\sin^2\frac{\pi i}{N}.$$

For $\beta = 0$, all normal modes oscillate independently and their energies E_i are constants of the motion. In the anharmonic case ($\beta > 0$), the normal modes are instead coupled and the variables Q_i no longer have simple sinusoidal oscillations.

Consider now the $\pi/2$ mode. For simplicity, we set $Q = Q_{\pi/2}$ and $P = P_{\pi/2}$. The equation of motion for the mode amplitude Q is [8]

$$\ddot{Q} = -2Q - 8\frac{\beta}{N}Q^3, \tag{4}$$

and the constant modal energy reads

$$E = \frac{1}{2}\left(P^2 + 2Q^2 + 4\frac{\beta}{N}Q^4\right). \tag{5}$$

We will excite this mode at $t = 0$ by setting $Q \neq 0$ and $P = \dot{Q} = 0$ always. For $\beta > 0$ the solution of Eq. (4), with initial conditions $Q(0) = Q_0$ and $\dot{Q}(0) = 0$, is

$$Q(t) = Q_0 \text{cn}(\Omega t; k^2), \tag{6}$$

where cn is the periodic Jacobi elliptic function with period $\tau = 4K(k)/\Omega$, $K(k)$ is the complete elliptic integral of the first kind, and, in terms of the energy density $\epsilon = E/N$,

$$Q_0^2 = \frac{N}{4\beta}(\sqrt{1 + 8\epsilon\beta} - 1), \quad k^2 = \frac{1}{2}\frac{\sqrt{1 + 8\epsilon\beta} - 1}{\sqrt{1 + 8\epsilon\beta}}, \tag{7}$$

and

$$\Omega^2 = \frac{2}{1 - 2k^2}. \tag{8}$$

The same formulas hold for $n = \frac{3}{4}N$, so the mode $3\pi/2$ behaves like the $\pi/2$ mode.

We observe that, due to symmetry constraints, for the OMSs other constants of the motion hold, besides the energy of the mode. For instance, one has

$$x_i + x_{i+1} = 0 \tag{9}$$

for the π mode and

$$x_i + x_{i+1} + x_{i+2} + x_{i+3} = 0 \tag{10}$$

for the $\pi/2$ mode.

As physical observables, for the analysis of the π mode we considered in [6] the quantities

$$\eta_i = x_i + x_{i+1}. \tag{11}$$

Here, for the $\pi/2$ mode, we consider the quantities

$$\eta_i(t) = x_i(t) + x_{i+1}(t) + x_{i+2}(t) + x_{i+3}(t), \quad i = 1, \dots, N, \tag{12}$$

and we study the distribution of their values when the system is unstable. Indeed, these quantities are always equal to zero during the time evolution of the system, if it is stable, independently of the choice of the initial condition $Q(0)$. Instead, when the system is not stable, the η_i's are different from zero and the distribution of their values depends on the exchange of energy among the $\pi/2$ and the other modes. The numerical results are independent of the choice of index i [3].

In recent years, a new theoretical framework, called nonextensive statistical mechanics, has appeared for describing the thermostatistics of systems typically exhibiting long-range correlations, (asymptotic) scale invariance, multifractality, etc. [16,17]. The nonextensive scenario generalizes the classical Boltzmann-Gibbs (BG) statistics in the sense that it applies to nonergodic, e.g., weakly chaotic, systems (for a regularly updated bibliography, see [18]). The entropy on which it is based reads

$$S_q = K \frac{1 - \sum_{i=1}^{W} p_i^q}{1-q} \left(S_1 \equiv S_{BG} = -K \sum_{i=1}^{W} p_i \ln p_i \right),$$

(13)

where W is the total number of microscopic states of the system. This entropy, under suitable constraints, is extremized by a q-Gaussian distribution. S_q is nonadditive, but for special values of the parameter q can be extensive, according to the prescription of Clausius [17]. Recently, a connection between generalized entropies and number theory has been found [19]. In particular, the entropy S_q has been related to the classical Riemann ζ function.

In a range of values of the energy density between the two thresholds ϵ_1 and ϵ_2, we show that the statistical distribution of the observables (12) is a q-Gaussian one for very long times. Precisely, the system reaches a weakly chaotic regime in a long-standing quasistationary state, for many different values of ϵ. For example, a quasistationary state is obtained for $N = 16$ and $\epsilon = 0.095$, with $q = 0.9255 \pm 0.0003$.

III. INTEGRATION OF THE EQUATIONS OF THE MOTION

The stability of the $\pi/2$ mode can be studied numerically by integrating the equations of motion without introducing external perturbation, as in [4,5,7]. The only perturbation introduced is due to computational errors of the algorithm of numerical integration. We have tested that these errors, which "trigger" the initial perturbation in the region of instability, remain very small and are completely negligible in the region of stability. We point out that the correctness of our method has been tested in three different contexts [5,7,8] with a very convincing agreement between numerical data and theoretical predictions.

The equations of motion in the variables x_i, p_i are integrated by means of a bilateral symplectic algorithm [20]. We recall that the dynamical properties of the FPU β system depend only on the product $\epsilon\beta$, so in all numerical experiments we put $\beta = 1$ and change the value of the energy density without loss of generality. We excite the nonlinear $\pi/2$ mode at $t = 0$, as described above, by setting $Q \neq 0$ and $P = \dot{Q} = 0$ always. We fix the initial value of the energy density ϵ and obtain the initial value of Q from Eq. (5) with $P = 0$; then, from inverse transformations of Eq. (1), the initial values of x_i and p_i are obtained, and the Hamilton equations are integrated in the variables x_i and p_i.

The scheme to obtain the distribution of the η_i, given by Eq. (12) is the following. Hereafter we choose $i = N/4$. For fixed (ϵ, N), we integrate the equations of motion with an integration step $\Delta t = 0.02$. After a transient of 2×10^8 integration steps, we calculate the value of the variable η_i

every 200 integration steps and we follow the evolution of the system for a time approximately equal to 4.2×10^9 integration steps, equivalent to approximately $84 \times 10^6/(\sqrt{2}\pi)$ periods of the corresponding linear mode ($\tau_{\pi/2} = \sqrt{2}\pi$). Longer integration times and shorter integration steps give qualitatively the same behavior. Then we consider the deviations $\xi_i = \eta_i - \langle \eta_i \rangle$ numerically obtained, and we determine the associated distribution $f(\xi_i)$. This distribution is compared with two theoretical distributions, namely, the Gaussian and the q-Gaussian distributions; the latter is defined by

$$f(\xi) = a[1 - (1-q)b^2\xi^2]^{1/(1-q)},$$

(14)

with

$$a = b\frac{\sqrt{q-1}\,\Gamma(1/(q-1))}{\sqrt{\pi}\,\Gamma((3-q)/[2(q-1)])} \quad \text{if} \quad 1 < q < 3,$$

(15)

$$a = b\frac{\sqrt{1-q}\,\Gamma(3/2 + 1/(1-q))}{\sqrt{\pi}\,\Gamma\left(\frac{q-2}{q-1}\right)} \quad \text{if} \quad q < 1.$$

(16)

Here Γ denotes the Euler Gamma function.

IV. NUMERICAL RESULTS

For the case $N = 16$, the values of the two stability thresholds are respectively $\epsilon_1 = 0.044\,655\,2$ and $\epsilon_2 = 0.135\,266\,73$. For $\epsilon = 0.135\,266\,74$ the $\pi/2$ mode is stable again. Just above ϵ_1, the behavior of the mode is not chaotic. As for the π mode, one observes recurrences, and the mode exchanges with the other modes only a small fraction of its energy, also for very long times. The irregularity of the $\pi/2$ mode increases on increasing the energy density, and for $\epsilon > 0.06$ the system becomes chaotic.

In Figs. 2 and 3, the numerical, Gaussian, and q-Gaussian distributions for $N = 16$ and $\epsilon = 0.135\,266\,73$ are shown. The q-logarithmic plot of the three distributions is normalized with the maximum value $f(0)$ of the numerical one, and is shown as a function of $[\xi f(0)]^2$. The χ^2 analysis gives an excellent agreement of the q-Gaussian with the numerical approximation.
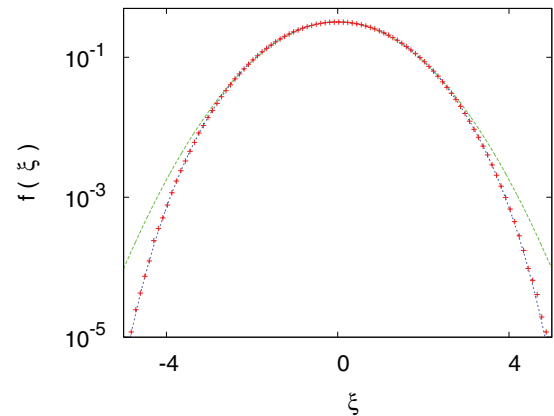

FIG. 2. (Color online) Log-linear representation of the numerical distribution $f(\xi)$ (red pluses), Gaussian distribution (green dashed upper curve), and q-Gaussian distribution (blue dotted curve) with $q = 0.9225 \pm 0.0007$, for $N = 16$ and $\epsilon = \epsilon_2 = 0.135\,266\,73$. We get $\chi_g^2 = 2.78 \times 10^{-4}$ and $\chi_{qg}^2 = 5.72 \times 10^{-7}$.
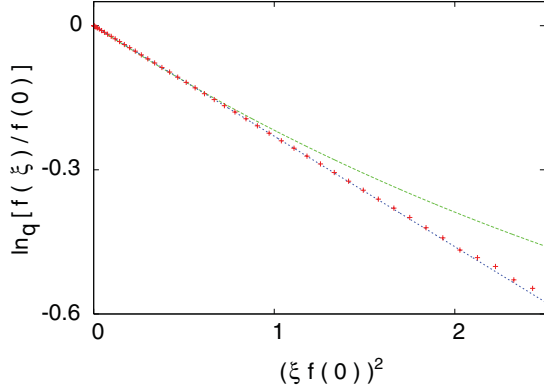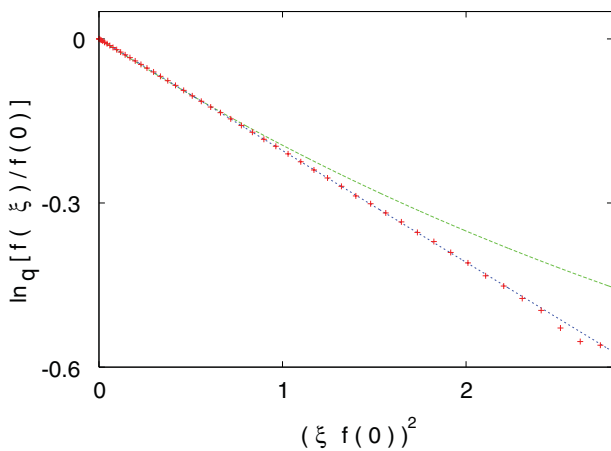
FIG. 3. (Color online) q-logarithmic vs square representation of the numerical distribution $f(\xi)$ (red pluses), Gaussian distribution (green dashed upper curve), and q-Gaussian distribution (blue dotted curve) shown in Fig. 2.

Hereafter we denote by χ_g^2 the χ^2 concerning the fit of the numerical distribution with the Gaussian distribution and by χ_{qg}^2 the same fit with the q-Gaussian one.

We have also considered many other values of (ϵ, N). Here we report only a few examples.

In Fig. 4 the three distributions are shown for $N = 16$ and $\epsilon = 0.095$. This value of the energy density is particularly relevant, since it corresponds to a state in which the stability time of the system has a minimum in the stability curve corresponding to $N = 16$. We hypothesize that the minimum is due to the presence of a maximum of the correlation between the modes. This would be coherent with the appearance of very stable q-Gaussian distributions. In Fig. 5 we report the distributions for $N = 128$ with $\epsilon = 0.06$, a value of energy density intermediate between the two stability thresholds. In Fig. 6 we show the three distributions for $N = 128$ with $\epsilon = 0.147\,155\,5$, just below the second threshold.
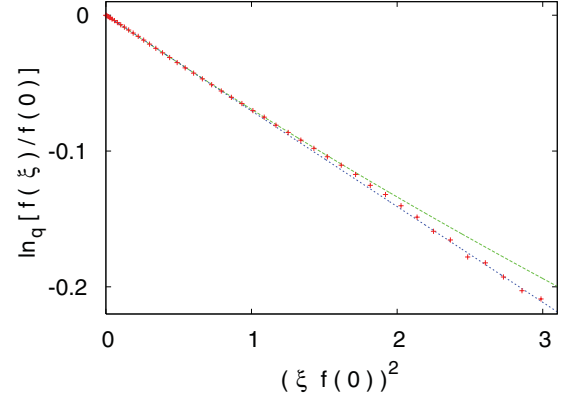

FIG. 4. (Color online) q-logarithmic vs square representation of the numerical distribution $f(\xi)$ (red pluses), Gaussian distribution (green dashed upper curve), and q-Gaussian distribution (blue dotted curve) for $N = 16$ and $\epsilon = 0.095$. We obtain $\chi_g^2 = 3.96 \times 10^{-4}$ and $\chi_{qg}^2 = 5.25 \times 10^{-6}$. The fitted value of q is 0.9318 ± 0.0008.

FIG. 5. (Color online) q-logarithmic vs square representation of the numerical distribution $f(\xi)$ (red pluses), Gaussian distribution (green dashed upper curve), and q-Gaussian distribution (blue dotted curve) for $N = 128$ and $\epsilon = 0.06$. We get $\chi_g^2 = 1.26 \times 10^{-5}$ and $\chi_{qg}^2 = 7.49 \times 10^{-6}$. The fitted value of q is 0.977 ± 0.003.

V. STUDY OF q AS A FUNCTION OF N

On increasing N, the fitted value of q tends to 1. In Fig. 7, the case $N = 256$ with $\epsilon = 0.1477$ is plotted. The theoretical distributions overlap with the numerical one.

As we have shown in [3], where we studied the dependence of the second threshold ϵ_2 on the number N, ϵ_2 tends asymptotically to a value ϵ_0 approximately equal to $0.147\,80$ for large values of N. This limit was checked up to $N = 4096$. In Fig. 8, we plot, as a function of $1/N$, both $(1 - q)$ and $\epsilon_0 - \epsilon$ where, for each value of N, ϵ is taken at the edge of the second threshold. We find that $q \to 1$ in the thermodynamic limit, as we expected in agreement with the metastability analysis of [21,22]. These quasistationary states appear as a *mesoscopic effect* for N not much larger than, say, 100.

Another crucial point consists in the time dependence of the parameter q. In Fig. 9 the behavior of q as a function of the integration time, for $\epsilon = 0.095$, is shown for $N = 16, 32$, and 64. The total number of iterations is 32×10^9, corresponding to an integration time of 6.4×10^8. In addition, in Fig. 10 we plot the three distributions at the end of the integration for $N = 16$
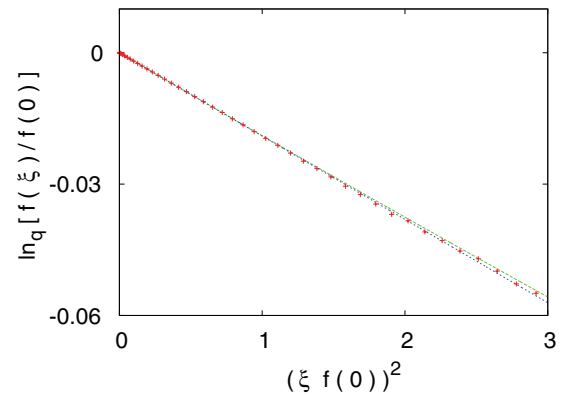

FIG. 6. (Color online) q-logarithmic vs square representation of the numerical distribution $f(\xi)$ (red pluses), Gaussian distribution (green dashed upper curve), and q-Gaussian distribution (blue dotted curve) for $N = 128$ and $\epsilon = 0.147\,155\,5$. We find $\chi_g^2 = 6.91 \times 10^{-7}$ and $\chi_{qg}^2 = 5.35 \times 10^{-7}$. The fitted value of q is 0.994 ± 0.001.
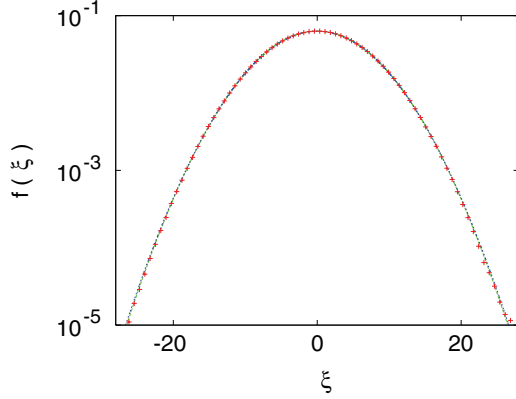
FIG. 7. (Color online) log-linear representation of the three distributions for $N = 256$ and $\epsilon = 0.1477$: Gaussian and q-Gaussian distributions overlap with the numerical one (red crosses). We get $\chi^2_g = 2.42 \times 10^{-7}$ and $\chi^2_{qg} = 2.21 \times 10^{-7}$.

and the same value of ϵ. The value of q stabilizes at $q = 0.9255 \pm 0.0003$. The best-fit curve is again a q-Gaussian, with very high accuracy. As in [23] we reach a quasistationary state in which our dynamical observables obey a q-Gaussian thermostatistics.

Regarding the error on the parameter q, we wish to remark that we integrate the equations of motion starting with initial conditions corresponding to an exact solution. Therefore, in order to evaluate the error on q it would not be adequate to average over different initial conditions. So we estimate the error on q by means of the fitting procedure. This estimation is confirmed by the fact that, for very long integration times (see Fig. 9), the value of q for fixed values of N and ϵ stabilizes with time. The variations observed, in the fourth decimal digit, are of the same order as the error obtained with the best-fit procedure.

On the other hand, what is relevant is that q is significantly different from 1 and tends to 1 for N very large, as we can see from the numerical results.
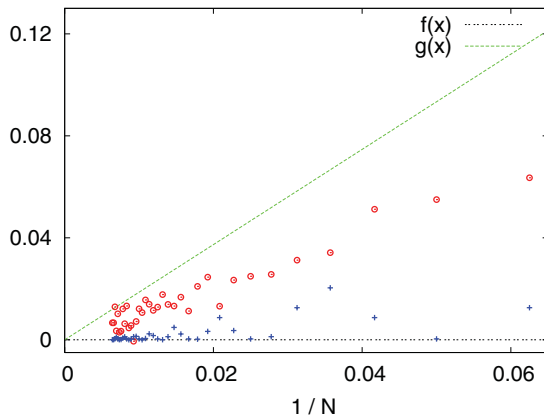

FIG. 8. (Color online) $(\epsilon_0 - \epsilon)$ (blue +) and $(1 - q)$ (red ○) vs $1/N$ [$\epsilon_0 = \lim_{N \to \infty} \epsilon_2(N)$]; ϵ is taken at the edge of the second threshold ϵ_2 for each value of N. Each red ○ corresponds to a blue + and indicates its value of q. The oscillations of the values of the blue + are due to the changes of ϵ_2 as a function of N (see Fig. 4 of Ref. [3]). The straight lines $y = 0$ [$f(x)$] and $y = 1.8671x$ [$g(x)$], between which all the values of q are distributed, are shown.
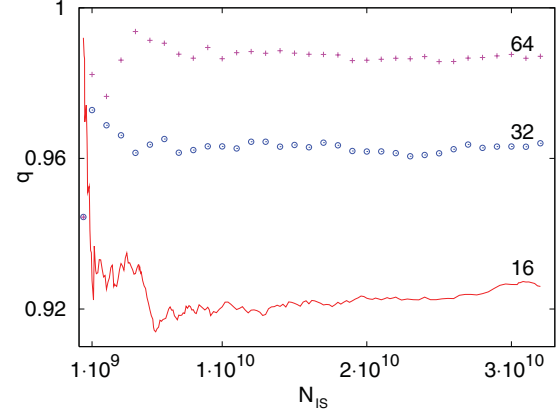

FIG. 9. (Color online) q vs the number of integration steps N_{IS} for $\epsilon = 0.095$, $N = 16$ (red solid curve), $N = 32$ (blue ○), and $N = 64$ (purple pluses). The integration time is $t = 0.02 N_{IS}$. The asymptotic values of q are respectively $q_{16} = 0.9255 \pm 0.0003$, $q_{32} = 0.9640 \pm 0.0004$, $q_{64} = 0.9871 \pm 0.0004$.

There is no evidence of the appearance, even after long times, of limit distributions different from q-Gaussians (in contrast with what occurs in the numerical study in [13] in a different energy-space region). Even for quite large values of N, the q-Gaussian is always an excellent fit distribution. Moreover, the energy density interval where this phenomenon is observed is not small, but of a sufficiently large size.

VI. FINAL REMARKS

A general result is that *the value of the parameter q is always less than* 1 for variable energy densities and tends to 1 with increasing N. This phenomenon also emerged in [23] for the sum of iterates of the sine-circle map. This feature is typical of the $\pi/2$ mode; indeed, in the case of the π mode our previous analysis [6] (as well as the recent one [13]) showed that $q > 1$.
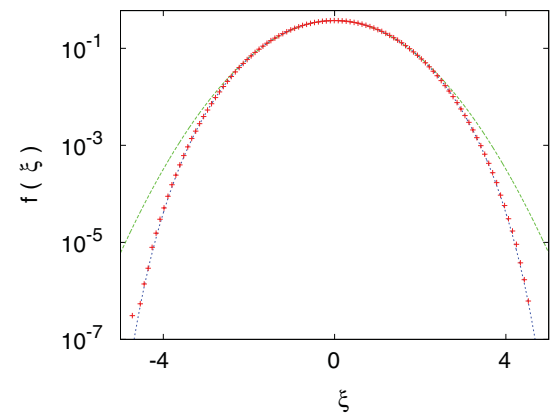

FIG. 10. (Color online) Log-linear representation of the numerical distribution $f(\xi)$ (red pluses), Gaussian (green dashed upper curve), and q-Gaussian distribution (blue dotted curve) for $N = 16$ and $\epsilon = 0.095$, after 32×10^9 iterations. We obtain $\chi^2_g = 4.50 \times 10^{-4}$ and $\chi^2_{qg} = 8.87 \times 10^{-7}$. The fitted value of q is 0.9255 ± 0.0003.

We conjecture that this reflects possibly different *roads to chaos*: values of $q > 1$ could be related to the fact that, with increasing ϵ, the system tends to a strong chaotic dynamics, whereas $q < 1$ could correspond to a different transition from chaos to order. Nonlinear dynamics can exhibit such effects. For example, the logistic map enters into chaos at the Feigenbaum point through a power law increasing with time ($q < 1$), whereas it enters through a power law decreasing with time ($q > 1$) at its tangent bifurcation point in the well-known cycle 3.

[1] E. Fermi, J. R. Pasta, and S. Ulam, in *Collected Papers of E. Fermi*, edited by E. Segré (University of Chicago Press, Chicago, 1965), Vol. II, p. 978.

[2] *The Fermi-Pasta-Ulam Problem: A Status Report*, edited by G. Gallavotti, Lecture Notes in Physics Vol. 728 (Springer, Berlin, 2008).

[3] M. Leo, R. A. Leo, and P. Tempesta, J. Stat. Mech. (2011) P03003.

[4] M. Leo and R. A. Leo, Phys. Rev. E **74**, 047201 (2006).

[5] M. Leo and R. A. Leo, Phys. Rev. E **76**, 016216 (2007).

[6] M. Leo, R. A. Leo, and P. Tempesta, J. Stat. Mech. (2010) P04021.

[7] A. Cafarella, M. Leo, and R. A. Leo, Phys. Rev. E **69**, 046604 (2004).

[8] P. Poggi and S. Ruffo, Physica D **103**, 251 (1997).

[9] S. Shinohara, Prog. Theor. Phys. Suppl. **150**, 423 (2003).

[10] G. M. Chechin, D. S. Ryabov, and K. G. Zhukov, Physica D **203**, 121 (2005).

[11] N. Budinsky and T. Bountis, Physica D **8**, 445 (1983).

[12] S. Flach, Physica D **91**, 223 (1996).

[13] C. Antonopoulos, T. Bountis, and V. Basios, Physica A **390**, 3290 (2011).

[14] A. Campa, T. Dauxois, and S. Ruffo, Phys. Rep. **480**, 57 (2009).

[15] M. Antoni and S. Ruffo, Phys. Rev. E **52**, 2361 (1995).

[16] C. Tsallis, J. Stat. Phys. **52**, 479 (1988).

[17] C. Tsallis, *Introduction to Nonextensive Statistical Mechanics—Approaching a Complex World* (Springer, New York, (2009).

[18] [http://tsallis.cat.cbpf.br/TEMUCO.pdf].

[19] P. Tempesta, Phys. Rev. E **84**, 021121 (2011).

[20] L. Casetti, Phys. Scr. **51**, 29 (1995).

[21] G. Benettin, A. Carati, L. Galgani, and A. Giorgilli, in *The Fermi-Pasta-Ulam Problem: A Status Report* (Ref. [2]), p. 151.

[22] D. Bambusi and A. Ponno, Commun. Math. Phys. **264**, 539 (2004).

[23] O. Afsar and U. Tirnakli, Phys. Rev. E **82**, 046210 (2010).